Journal of Medicinal Chemistry

Article

pubs.acs.org/jmc

Noncyclam Tetraamines Inhibit CXC Chemokine Receptor Type 4 and Target Glioma-Initiating Cells

Laia Ros-Blanco,[†] Judit Anido,[‡] Ramon Bosser,[§] José Esté,[∥] Bonaventura Clotet,[∥] Ana Kosoy,[§] Luis Ruíz-Ávila,[§] Jordi Teixidó,[†] Joan Seoane,*[,‡] and José I. Borrell*[,†]

[†]Grup d'Enginyeria Molecular, Institut Químic de Sarrià, Universitat Ramon Llull, Via Augusta 390, E-08017 Barcelona, Spain

[‡]Translational Research Program, Vall d'Hebron Institute of Oncology (VHIO), Vall d'Hebron University Hospital, E-08035 Barcelona, Spain and Universitat Autònoma de Barcelona, E-08193 Cerdanyola del Vallès, Spain

[§]Janus Development SL, Parc Científic Barcelona, Baldiri Reixac 10-12, E-08028 Barcelona, Spain

[∥]IrsiCaixa, Hospital Universitari Germans Trias i Pujol, Universitat Autònoma de Barcelona, E-08916 Badalona, Spain

Supporting Information

ABSTRACT: The three stereoisomers of the noncyclam compound **1** (**1**(*R*,*R*), **1**(*S*,*S*), and the *meso* form **1**(*S*,*R*)) and their corresponding tetrahydrochlorides **11** were prepared from (*S*)- and (*R*)-2-methylpiperidine. We have evaluated their inhibitory activity on the CXC chemokine receptor type 4 (CXCR4), toxicity properties, and assessment of their effect on glioma initiating cells (GICs) in comparison with the prototype compound AMD3100. The IC_{50} values determined on human recombinant (CHO) cells showed very similar inhibitory activities albeit a lower K_B for AMD3100, with the **1**(*R*,*R*) isomer being second in potency. All the compounds showed low cardiac toxicity but, contrary to AMD3100, gave maximum nonlethal doses of around 2.0 mg/kg. The CXCR4 inhibitors had an effect on the state of differentiation of GICs, decreasing the percentage of CD44+ cells in glioblastoma multiform neurospheres in vitro. Moreover, these CXCR4 inhibitors blocked the capacity of cells to initiate orthotopic tumors in immunocompromised mice.

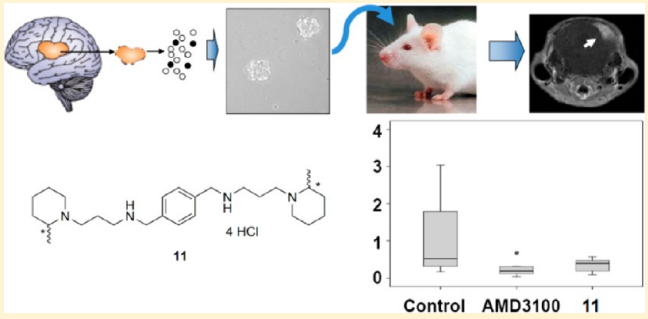

INTRODUCTION

Gliomas have morphologic and gene-expression characteristics similar to glia, the support cells of the brain, and they include astrocytomas, oligodendrogliomas, mixed oligoastrocytomas, and ependimomas according to their histological characteristics. Gliomas can be divided into four clinical grades on the basis of their histology and prognosis. Grade IV gliomas (glioblastoma, GBM) either arise de novo or progress from lower grade to higher grade over time; the tumor of patients originally diagnosed with a lower grade will often progress to a GBM. Histologically, GBMs exhibit microvascular hyperproliferation and/or necrosis, which normally is surrounded by densely packed tumor cell nuclei referred to as being pseudopalisades.[1] GBMs have a propensity to infiltrate throughout the brain, and this invasive nature results in the inability of surgery to completely cure patients. GBMs are highly malignant, are usually recalcitrant to radio- and chemotherapy, and have a median survival of 1−2 years.[2,3] Novel molecular-targeted therapies against these devastating tumors are required.

Recently, a subpopulation of tumor cells with stem-cell-like properties has been identified in gliomas. These cells, called glioma stem cells or glioma-initiating cells (GICs), are characterized by their self-renewal capacity, their multilineage differentiation properties, their high oncogenic potential, and their ability to generate detached spherical cellular structures (neurospheres) when cultured in serum-free medium. Several markers, most of them previously described for neuroprogenitor cells, have been reported to identify GICs. Specifically, we and others have shown that a glioma subpopulation of cells expressing the cell surface protein, CD44, are enriched for cancer stem cells.[4] GICs are considered to be responsible for the initiation, propagation, and recurrence of tumors. Moreover, GICs are resistant to standard therapy. This indicates that GICs are critical therapeutic targets and that more effective therapies will result from approaches aimed at targeting the stem-cell-like component of gliomas.[5]

Our work in the field of anti-HIV entry/fusion inhibitors[6,7] led to the identification of novel potent HIV-1 entry CXCR4 coreceptor inhibitors targeting CXCR4 coreceptor without cytotoxicity at the tested concentrations.[8] Among them, compound **1** (Chart 1) was selected as a lead compound because it presents nearly the same level of activity as the reference compounds, **1** (EC_{50} = 0.019 μM) and the bicyclam AMD3100 (**2**, Plerixafor, EC_{50} = 0.002 μM), and shows no cell toxicity at the tested concentrations of up to 25 μg mL^{-1}.

Received: April 19, 2012
Published: August 21, 2012

Chart 1. Noncyclam CXCR4 Inhibitor 1, AMD3100 (2), and Stereoisomers of Compound 1

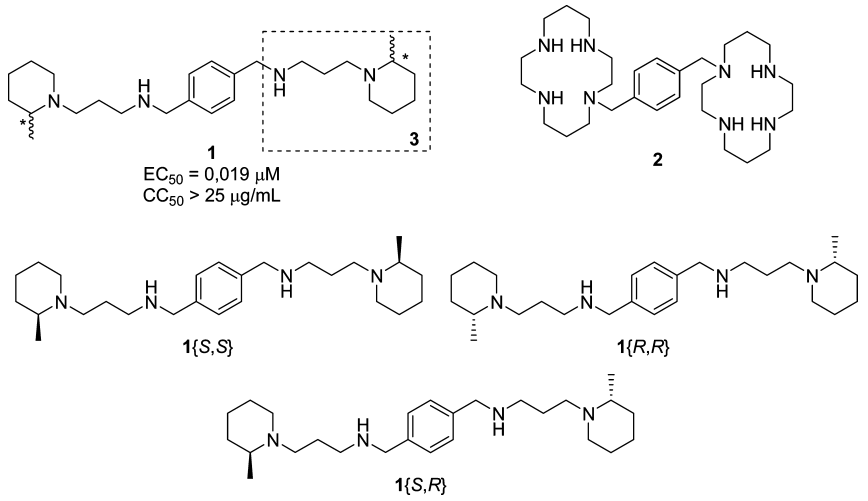

Scheme 1. Synthesis of the Three Stereoisomers of Compound 1 (1(*R*,*R*), 1(*S*,*S*), and the *meso* Form 1(*S*,*R*)) and the Corresponding Tetrahydrochlorides 11(*R*,*R*), 11(*S*,*S*), and 11(*S*,*R*)

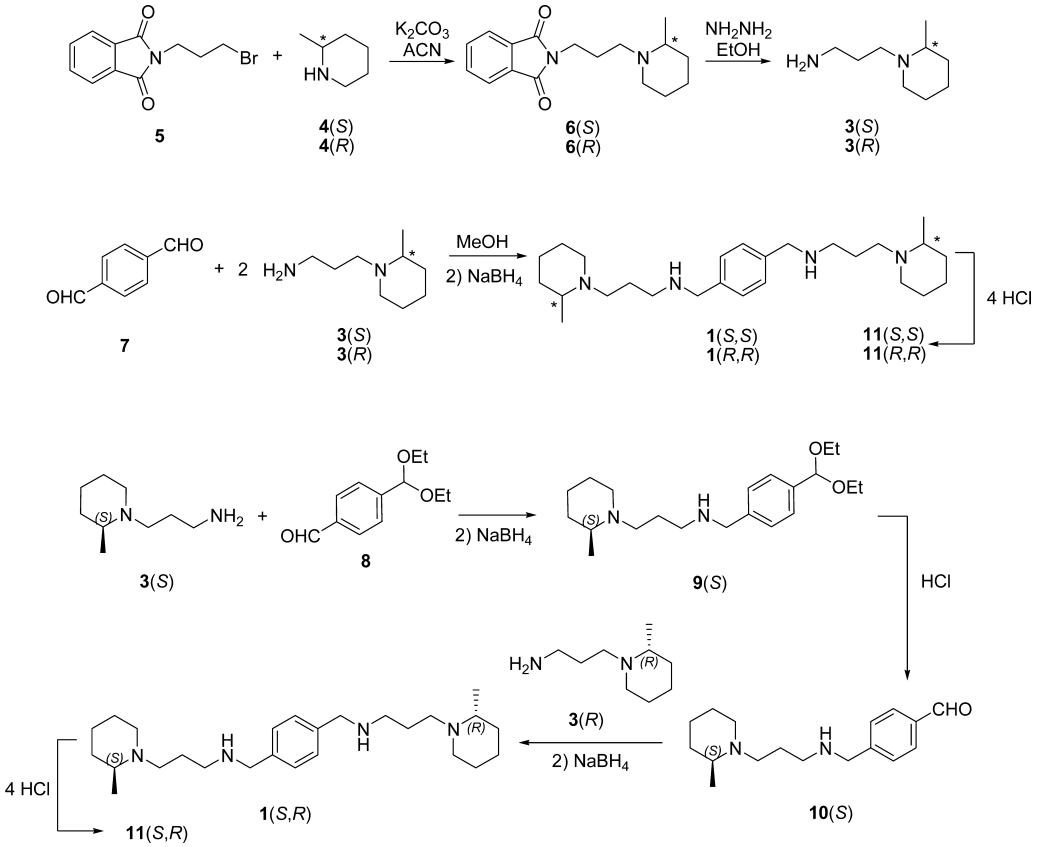

Compound **1** was obtained and tested as a mixture of three stereoisomers (**1**(*R*,*R*), **1**(*S*,*S*), and the *meso* form **1**(*S*,*R*) in an approximate 25:25:50 ratio) due to the presence of two chiral centers introduced from the racemic precursor *N*-(3-aminopropyl)-2-pipecoline (**3**).

CXCR4 is a transmembrane receptor that regulates the trafficking and homing of various cell types including stem cells and cancer stem cells. CXCL12 is the ligand of CXCR4 and upon binding to CXCR4 engages several signal transduction pathways including the MAPK and the PI3K-Akt pathways. CXCR4 expression in glioma confers poor prognosis after surgery,[9] and CXCR4 blockade in mice delays tumor recurrence after irradiation by inhibiting the recruitment of CD11b+ monocytes/macrophages that participate in revascularizing the tumor.[10] These results suggest a critical role of CXCR4 in glioma. In addition, there is much evidence that demonstrates the involvement of the CXCL12/CXCR4 pathway in different cell functions critical for glioma development. Among others, the CXCL12/CXCR4 pathway[11] promotes tumor vasculogenesis and angiogenesis in tumor stem-like glioma cells.[12] Similarly, the pathway increases cell motility and proliferation in the U-118 human glioma cell line.[13] In addition, the blockage of CXCR4

dx.doi.org/10.1021/jm300862u | J. Med. Chem. 2012, 55, 7560−7570

induced a significant increase in apoptosis. Taken all together, these results point to CXCR4 as a promising therapeutic target in glioma. Because of the described function of CXCR4 in cancer and stem cells, CXCR4 antagonists could be effective against cancer-initiating cells and, hence, tumor initiation and relapse.

We systematically isolate cancer-initiating cells from patient-derived glioma samples, glioma initiating cells (GICs) that we culture and study. GICs grow as neurospheres in culture and can be expanded by serial passaging. In addition, patient-derived GICs are inoculated in the brain of NOD-SCID mice. Tumors arising from GICs maintain the same characteristics as the original human tumor.[14]

Here we report the synthesis of the three stereoisomers of compound **1** (**1**(*R,R*), **1**(*S,S*), and the *meso* form **1**(*S,R*)), the evaluation of their compared inhibitory activity on the CXCR4 coreceptor, the evaluation of their toxicity properties, and the assessment of their effect on GICs and glioma initiation in comparison with AMD3100.

RESULTS AND DISCUSSION

Synthesis. To obtain the three stereoisomers of compound **1** (**1**(*R,R*), **1**(*S,S*), and the *meso* form **1**(*S,R*)), it was first necessary to prepare the homochiral amines **3**(*S*) and **3**(*R*), because the diamine **3** is only commercially available as the racemic mixture. The Gabriel protocol was selected for the synthesis of **3**(*S*) and **3**(*R*) starting from the corresponding enantiomeric 2-methylpiperidines **4**(*S*) and **4**(*R*) (Scheme 1). Although the resolution of 2-methylpiperidine (**4**) has been described,[15] finally we used commercially available (*S*)-2-methylpiperidine (**4**(*S*)) and (*R*)-2-methylpiperidine (**4**(*R*)) with purities of 97%, the latter one as the HCl salt.

As for the nucleophilic substitution of the bromine atom present in the commercially available *N*-(3-bromopropyl)-phthalimide (**5**), we initially considered the same reaction conditions we have used for the synthesis of similar diamines: an excess of the corresponding cyclic amine in acetone at reflux for 12 h.[16] However, in the case of **4**(*S*) and **4**(*R*), we considered a better approach to use stoichiometric amounts of the chiral amines to minimize their amount and avoid intermediate purifications. A bibliographic search revealed a modification of this protocol described by Jo et al. in which the use of solid K_2CO_3 to capture HBr formed allows one to use a 1.2:1 ratio between the chiral amine **4** and the bromo-substituted phthalimide **5** (or even use stoichiometric amounts).[17] Furthermore, the use of acetonitrile as solvent allows reducing by half the reaction time (although we preferred to maintain the reflux for 8 h to ensure the total conversion of the reagents). In such modification the hydrolysis of the alkylated intermediates **6**(*S*) and **6**(*R*) was performed under more mild conditions using hydrazine in EtOH instead of 6 M aqueous HCl.

Using such methodology, the 2-methylpiperidines **4**(*S*) and **4**(*R*) were converted to the alkylated intermediates **6**(*S*) and **6**(*R*) in 92% and 97% yields, respectively, which were hydrolyzed to the desired homochiral *N*-(3-aminopropyl)-2-pipecolines **3**(*S*) and **3**(*R*) in 79% and 73% yields, respectively (total yields greater than 60%).

The synthesis of the stereoisomers **1**(*S,S*) and **1**(*R,R*) was carried out following the methodology previously described by our group for **1**.[8] Thus, the treatment of terephthaldehyde (**7**) with 2 equiv of the corresponding amine **3**(*S*) and **3**(*R*) in anhydrous MeOH at reflux for 24 h in the presence of anhydrous Na_2SO_4 as the dehydrating agent, followed by filtration and cooling of the resultant filtrate to 0 °C, addition of 2 equiv of $NaBH_4$, and stirring for 24 h at room temperature, afforded **1**(*S,S*) and **1**(*R,R*) as yellow oils in 97% and 83% yields, respectively (Scheme 1).

In the case of the *meso* form **1**(*S,R*), being an asymmetrically substituted compound, it was necessary to use the monoprotected terephthaldehyde **8** as previously described by our group.[8] Although the reductive amination could be initiated either by using **3**(*S*) or **3**(*R*) at first, we preferred to start with **3**(*S*) since it was more readily available because it proceeds from the more commercially accessible (*S*)-2-methylpiperidine (**4**(*S*)). Thus, the reductive amination of **8** with 1 equiv of **3**(*S*) in the same reaction conditions described above for the synthesis of the symmetrical compounds afforded **9**(*S*) in 84% yield. **9**(*S*) was subsequently hydrolyzed to the aldehyde **10**(*S*) with 2 M HCl in 80% yield, which was treated with 1 equiv of **3**(*R*) in the same reductive amination conditions to afford the *meso* form **1**(*S,R*) in 83% yield (56% yield from **8**) (Scheme 1).

The resulting stereoisomers **1**(*R,R*), **1**(*S,S*), and the *meso* form **1**(*S,R*) were converted into the corresponding tetrahydrochlorides **11**(*R,R*), **11**(*S,S*), and **11**(*S,R*) upon treatment with HCl in MeOH in almost quantitative yields. Finally, we obtained **1** and its tetrahydrochloride **11** as the mixture of the three stereoisomers (**1**(*R,R*), **1**(*S,S*), and the *meso* form **1**(*S,R*)) for comparison purposes by following the procedure previously described by our group.[8]

Antiviral Activity. As a first way to compare the biological activity in front of the CXCR4 receptor of compounds **11**(*R,R*), **11**(*S,S*), and **11**(*S,R*) and establish possible differences that can favor one candidate over the others, we decided to evaluate the anti-HIV activity (EC_{50}) and cytotoxicity (CC_{50}) in CXCR4+ MT-4 cells.

The results shown in Table 1 demonstrate that there are no significant differences between the three isomers, at least in this test. Consequently, we decided to work in parallel with **11**(*R,R*), **11**(*S,S*), and **11**(*S,R*) in the following experiments.

Table 1. Anti-HIV Activity (EC_{50}) and Cytotoxicity (CC_{50}) Measurements in MT-4 Cells of Tetrachlorohydrates 11, 11(*R,R*), 11(*S,S*), and 11(*S,R*)

compd	EC_{50}	CC_{50}
11	0.130 ± 0.04 μM	>44 μM
11(*R,R*)	0.125 ± 0.04 μM	>44 μM
11(*S,S*)	0.137 ± 0.06 μM	>44 μM
11(*S,R*)	0.139 ± 0.03 μM	26 ± 10 μM

ADME-TOX Studies. Since AMD3100 reported cardio toxicity, we were interested in comparing our products with AMD3100 in terms of cardio toxicity and affinity for the CXCR4 receptor. Therefore, both an in vitro CXCR4 antagonist effect assay and a conventional K+ Channel patch-clamp assay were performed for **11**(*R,R*), **11**(*S,S*), and **11**(*S,R*) and AMD3100. The antagonist effects of AMD3100, **11**(*R,R*), **11**(*S,S*), and **11**(*S,R*) on the CXCR4 receptor were determined using human recombinant (CHO) cells following the protocol described by Zhou et al.[18] The results obtained are shown in Figure 1. The IC_{50} values obtained for AMD3100, **11**(*R,R*), **11**(*S,S*), and **11**(*S,R*) indicate that these compounds present very similar inhibitory activities although the K_B (Dissociation constant) is lower for AMD3100, meaning this compound binding with the CXCR4 receptor is stronger than the others tested. The *R,R* isomer of **1** was second in terms of potency. For the cardiac toxicity determination, a conventional electrophysiological assay

dx.doi.org/10.1021/jm300862u | J. Med. Chem. 2012, 55, 7560−7570

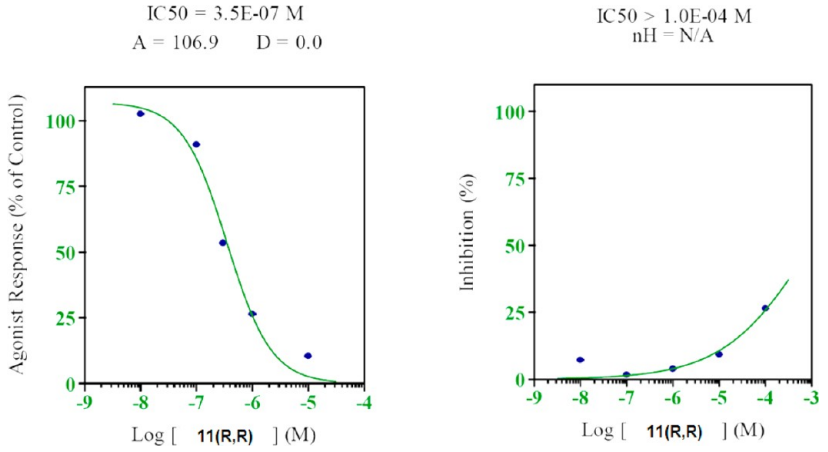

Figure 1. Antagonist effect and its related inhibition determination curves for **11**(*R,R*).

using whole cell patch-clamp technique proposed by Mathes[19] to study effects of the compounds on the hERG channel, was used. Briefly, CHO-K1 cells stably expressing hERG channel were used and compounds were valuated at 5 concentrations to determine the amplitude of hERG potassium channel tail currents. The percentage inhibition of the tail current by each compound is summarized in Table 2, showing that all of the compounds had low cardiac toxicity.

Table 2. Effect in the in Vitro Human CXCR4 Receptor Functional of Compounds AMD3100, 11(*R,R*), 11(*S,S*), and 11(*S,R*)

compd	IC_{50}	K_B	IC_{50} (hERG)
AMD3100	0.26 μM	0.077 μM	>100 μM
11(*R,R*)	0.35 μM	0.11 μM	>100 μM
11(*S,S*)	1.1 μM	0.32 μM	N.C.[a]
11(*S,R*)	0.79 μM	0.24 μM	>100 μM

[a]N.C. = IC_{50} value not calculable. Concentration−response curve shows less than 25% effect at the highest tested concentration.

To complement such data, we decided to study the acute intravenous toxicity in mice by determining the maximum nonlethal dose and the minimum lethal dose. The acute toxicities of the test items AMD3100, **11**(*R,R*), **11**(*S,S*), and **11**(*S,R*) were evaluated after their intravenous administration to Hsd:ICR (CD-1) mice, followed by an observation period of 14 days. In the study, 4 groups consisting of 4 animals (2 males and 2 females) each were administered in physiological saline solution at the doses between 1.0 and 4.0 mg/kg.

Viability/mortality and clinical signs were recorded daily during the acclimatization and during the first 30 min and at approximately 1, 2, 3, and 5 h after administration on test day 1. Viability/mortality was observed twice daily, and clinical signs were observed once daily during days 2−15. Body weights were recorded once during the acclimatization, on days 1 and 14, and before sacrifice (day 15). At the end of the observation period, all surviving animals and those that were found dead were necropsied, and a macroscopic examination was performed on the principal organ systems and tissues to record any macroscopic alterations related to the treatment.

No mortality was recorded in animals administered with AMD3100 at any dose level (1, 2, 3, 3.5, and 4 mg/kg). All animals administered with **11**(*S,R*) at 3.0 mg/kg, one male administered with **11**(*S,S*) at 2.0 mg/kg, and one female administered with **11**(*R,R*) at 2.5 mg/kg died immediately or within 1 min of administration.

On the basis of the results obtained, the maximum nonlethal dose and the minimum lethal dose of the test items when administered intravenously to Hsd:ICR (CD-1) mice for both sexes as well as for males and females separately were as follows: AMD3100 (as no mortality was recorded, it was considered that the minimum lethal dose is >4.0 mg/kg); **11**(*S,S*) (both sexes: maximum nonlethal dose, 1.5 mg/kg; minimum lethal dose, 2.0 mg/kg); **1**(*R,R*) (both sexes: maximum nonlethal dose, 2.0 mg/kg; minimum lethal dose, 2.5 mg/kg); **11**(*S,R*) (both sexes: maximum nonlethal dose, 2.5 mg/kg; minimum lethal dose, 3.0 mg/kg). The results obtained once more indicate that there are not significant differences between the tetrahydrochlorides **11**(*R,R*), **11**(*S,S*), and **11**(*S,R*) but pointed to a higher toxicity in vivo of these compounds with respect to AMD3100.

Effect of CXCR4 Inhibitors on GICs and Glioma Initiation. As a first step, to address the effect of CXCR4 inhibitors on patient-derived neurospheres, we decided to assess how the compounds affected the signaling pathways that are downstream of the CXCR4 receptor (the Akt and MAPK pathways). First of all, we decided to determine whether the ligand of the CXCR4 receptor, CXCL12, could induce the Akt and MAPK pathways in our cells. Treatment of neurospheres from three different patients (*GBM1*, *GBM2*, and *GBM3*) with CXCL12 slightly increased phospho-Akt (p-Akt) in GBM1 and GBM2 but not in GBM3. There was no major effect of CXCL12 treatment on phospho-MAPK (p-MAPK) (Figure 2). Two bands were detected in the p-MAPK blot corresponding to p44 and p42 MAPK. Both kinases share many functional roles; however, some specific functions have been assigned to each of them.[20]

We next decided to compare the effect of the CXCR4 inhibitors on the Akt and MAPK pathways using two different concentrations of compound (1 μM and 100 nM). To perform this experiment we decided to focus our studies on GBM2, the patient-derived neurospheres where CXCL12 was having some effect on p-Akt (see Figure 2). **11**(*S,R*) (ASR226) (at 1 μM) was the only compound that had a slight effect on p-Akt and, interestingly, in total Akt. No major effect was observed on p-MAPK in any of the conditions (Figure 3).

We repeated the same experiment treating the cells with the inhibitory compounds (at 1 μM) in the presence or absence of CXCL12. In this experiment, the effect of CXCL12 was not evident. However, and again, a minor effect of **11**(*S,R*) on p-Akt

dx.doi.org/10.1021/jm300862u | J. Med. Chem. 2012, 55, 7560−7570

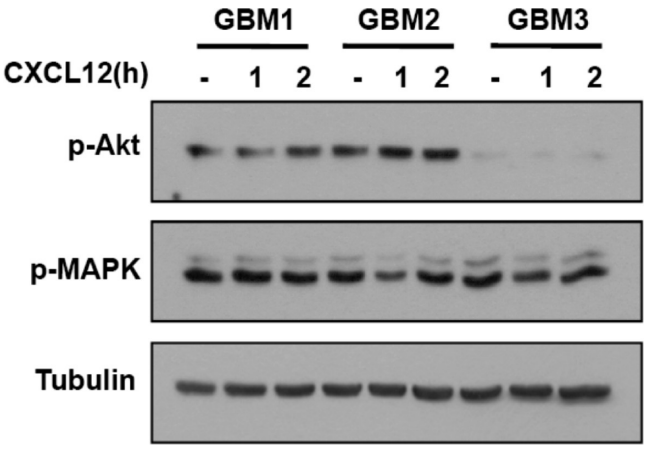

Figure 2. MAPK and Akt pathway activation by CXCL12. Neurospheres were dissociated and counted, and an equal number of cells were seeded. After 24 h of EGF, FGF, and B27 starvation, cells were treated with 100 mg/mL of CXCL12 during 1 or 2 h. Levels of p-MAPK, p-Akt, and Tubulin were determined by immunoblotting.

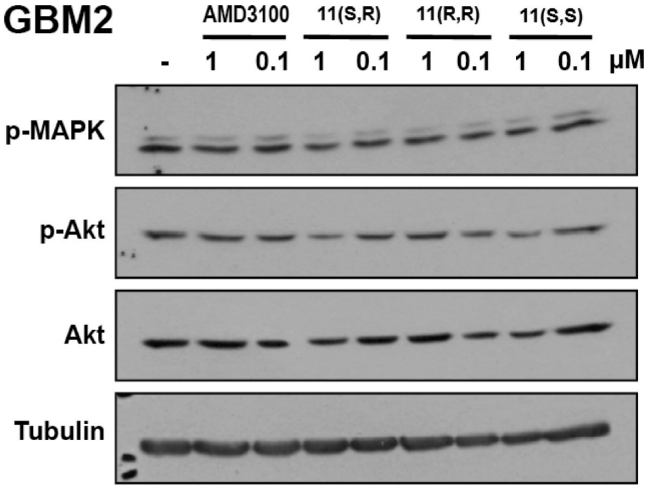

Figure 3. MAPK and Akt pathway inhibition by CXCR4 inhibitors AMD3100, **11**(*R,R*), **11**(*S,S*), and **11**(*S,R*). GBM2 neurospheres were dissociated, counted and an equal number of cells were seeded. Cells were treated or left untreated with CXCR4 inhibitors (1 μM) during 8 h. Levels of MAPK, p-Akt, Akt and Tubulin were determined by immunoblotting.

and total Akt was observed. Moreover, a slight decrease of p-MAPK was observed in cells treated with **11**(*S,S*) (Figure 4).

In summary, our data indicated that 1 μM **11**(*S,R*) had a minor effect on the Akt pathway whereas the rest of the compounds including the commercially available AMD3100 did not have a major effect on the Akt and MAPK pathways. At this point, we decided to assess the effect of the compounds on cell viability and proliferation. To this aim, we treated neurospheres from three patients with the compounds in the presence or absence of CXCL12. After 7 days of treatment, cells were counted. The number of cells after treatment is the result of a balance between the rate of proliferation and the rate of cell death. No major effect was observed in the conditions assayed; all drugs gave >80% viability with the exception of AMD3100, which gave ~65% with GBM1, indicating that the compounds do not have a major effect on cell proliferation nor viability.

We next decided to assess the effect of CXCR4 inhibitors on the state of differentiation of GICs. To determine the state of

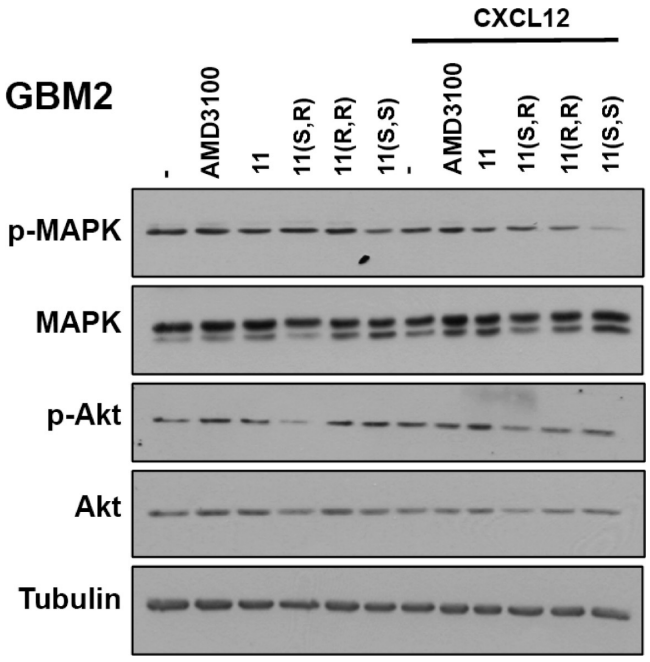

Figure 4. MAPK and Akt pathway inhibition by CXCR4 inhibitors in the presence of CXCL12. GBM2 neurospheres were dissociated and counted. After 24 h of EGF, FGF and B27 starvation cells were treated or left untreated with 1 μM CXCR4 inhibitors AMD3100, **11**, **11**(*R,R*), **11**(*S,S*), and **11**(*S,R*) during 8 h and/or CXCL12 (100 ng/mL) during 1 h. Levels of p-MAPK, MAPK, p-Akt, Akt, and Tubulin were determined by immunoblotting.

differentiation, we analyzed the levels of CD44, a well-described marker of cancer-initiating cells. We treated GBM neurospheres obtained from two GBM patients with the CXCR4 inhibitors (AMD3100, **11**, **11**(*R,R*), **11**(*S,S*), and **11**(*S,R*)) and analyzed the levels of CD44 by flow cytometry. The percentage of cells that did not express CD44 (*CD44 null*) increased in GBM neurospheres from two different patients treated with the CXCR4 inhibitors (Figure 5 and Supporting Information). As a consequence, the ratio CD44 low/CD44 null decreased in the presence of the CXCR4 inhibitors (Figure 5, bar graphs), indicating that the CXCR4 inhibitors decreased the amount of glioma-initiating cells, most likely inducing cell differentiation.

To confirm the effect of CXCR4 inhibition on glioma-initiating cells, we decided to perform an in vivo experiment. For this purpose, we used a glioma model that reproduces the tumor from the patient in mice described in our previous publication by Peñuelas et al. (Figure 6).[14]

We treated GBM neurospheres in culture with AMD3100 and **11**, the tetrahydrochloride of the mixture of the three stereoisomers (**1**(*R,R*), **1**(*S,S*), and the *meso* form **1**(*S,R*)), for 7 days. Then we inoculated in the brain of NOD-SCID mice using a stereotactic apparatus the same number of live cells, as analyzed by trypan blue staining, which were pretreated with the indicated compounds. Forty days after inoculation, we monitored tumor growth through magnetic resonance imaging (MRI). Images from the entire mouse brain were obtained, and tumor volume was quantified (Figure 7). Tumors generated from the cells pretreated with the CXCR4 inhibitors generated smaller and fewer tumors than control cells, confirming that the inhibition of CXCR4 prevents tumor initiation through the decrease of the number of glioma-initiating cells.

dx.doi.org/10.1021/jm300862u | *J. Med. Chem.* 2012, 55, 7560−7570

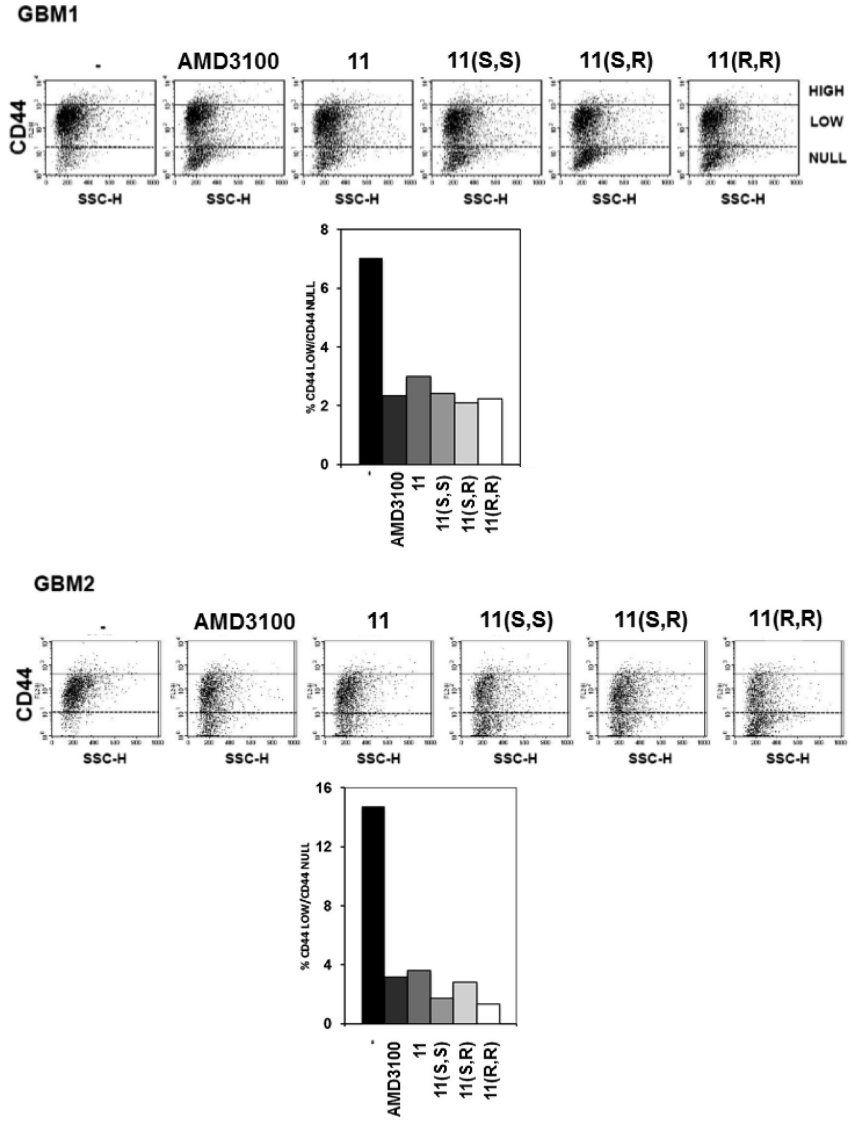

Figure 5. Effect of CXCR4 inhibitors on the CD44+ cell population in patient-derived GBM neurospheres. GBM neurosphere cultures were dissociated and counted, and an equal number of cells were seeded. Cells were treated with 1 μM of the indicated inhibitors (AMD3100, **11**, **11**(*R,R*), **11**(*S,S*), and **11**(*S,R*)) for 7 days. The percentage of cells expressing CD44 was determined by flow cytometry. Bar graphs show the ratio of CD44 low/CD44 null cells quantified by flow cytometry in the different conditions.

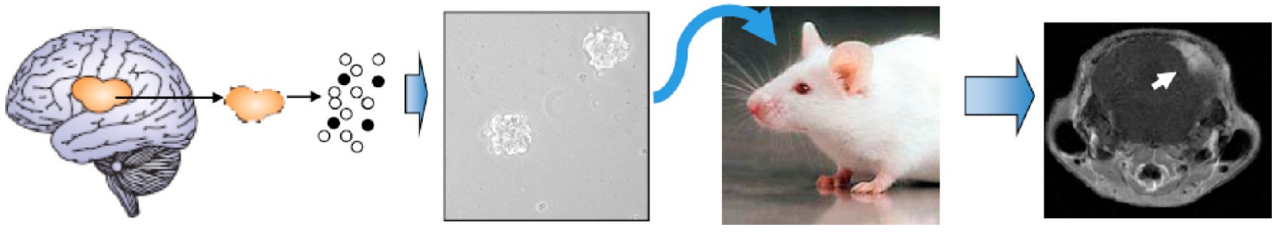

Figure 6. Scheme of mouse model for human glioblastoma.

Our results show that CXCR4 inhibition did not have a major effect on the PI3K-Akt and the MAPK pathways in contrast to those by Rubin et al.[21] However, both results may not be comparable because Rubin et al. used U87 and Dacoy, two regular cell lines, whereas we used fresh patient-derived cells. The models are different because, first, established cell lines have been cultured in artificial conditions for a long time diverging from the characteristics of a real tumor and, second, our cells are undifferentiated and enriched in GICs.

CONCLUSION

We obtained the three stereoisomers of compound **1**, **1**(*R,R*), **1**(*S,S*), and the *meso* form **1**(*S,R*), starting from the commercially available (*S*)-2-methylpiperidine (**4**(*S*)) and (*R*)-2-methylpiperidine (**4**(*R*)) in good overall yields by following our general methodology for the preparation of such tetraamines.[8] The anti-HIV activity (EC_{50}) and cytotoxicity (CC_{50}) in MT-4 cells of the corresponding tetrahydrochlorides, **11**(*R,R*), **11**(*S,S*), and **11**(*S,R*), were evaluated in comparison to compounds **11** (the

dx.doi.org/10.1021/jm300862u | J. Med. Chem. 2012, 55, 7560−7570

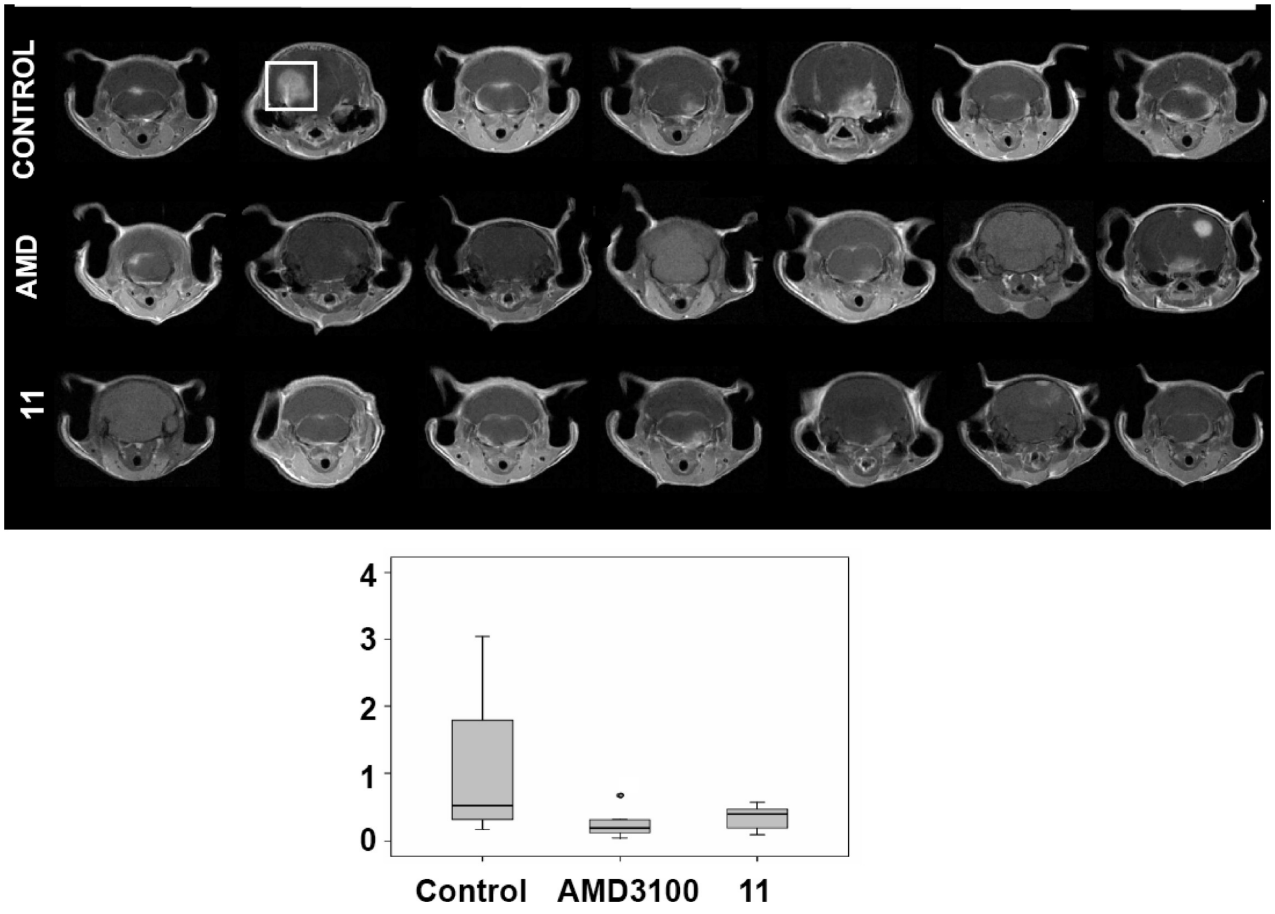

Figure 7. Effect of CXCR4 inhibitors AMD3100 and **11** on tumor growth. GBM1 neurospheres were dissociated and counted, and the same number of living cells was inoculated in the brain of NOD-SCID. Forty days after inoculation, the tumor size was determined through MRI and the tumor volume was quantified. The white box indicates an example of tumor detected by MRI.

tetrahydrochloride of the mixture of the three stereoisomers) and AMD3100. There were no significant differences between the three isomers. Furthermore, the IC_{50} values of AMD3100, **11**(*R,R*), **11**(*S,S*), and **11**(*S,R*) were determined on human recombinant (CHO) cells showing that these compounds presented very similar inhibitory activities, although the K_B was lower for AMD3100, with the **11**(*R,R*) isomer being second in potency.

Toxicity studies for AMD3100, **11**(*R,R*), **11**(*S,S*), and **11**(*S,R*) were carried out to assess the safety of such compounds for possible use in humans. All compounds tested induced low cardiac toxicity. The evaluation of the acute intravenous toxicity in mice showed that no mortality was recorded in animals administered with AMD3100 at any dose level, but compounds **11**(*R,R*), **11**(*S,S*), and **11**(*S,R*) gave a maximum nonlethal dose of ~2.0 mg/kg.

We found that these CXCR4 inhibitors affect the state of differentiation of GICs, decreasing the percentage of CD44+ cells in GBM neurospheres in vitro. Moreover, and expected based on the effect on the CD44+ cells, CXCR4 inhibitors prevent the capacity of cells to initiate orthotopic tumors in immunocompromised mice. Our results indicate that the CXCR4 inhibitors tested could be effective against GICs, preventing tumor initiation and recurrence and most likely metastasis in other tumor types.

EXPERIMENTAL SECTION

Chemistry. Commercial reagents (Fluka, Aldrich) were used without purification. The (*S*)-2-methylpiperidine (**4**(*S*)) and the (*R*)-2-methylpiperidine (**4**(*R*)), this later as hydrochloride, were purchased from Aldrich (Cat. no. 522902) and Astatech USA (Cat. no. 64253), respectively. IR spectra were recorded in a Nicolet Magna 560 Fourier transform infrared (FTIR) spectrophotometer. Wavenumbers (ν) are expressed in cm^{-1}. ^1H and ^{13}C NMR spectra were recorded in a Varian Gemini 300HC instrument (operating at a field strength of 300 and 75.5 MHz, respectively) or a Varian Gemini 400-MR instrument (^1H NMR 400 MHz and ^{13}C NMR 100.6 MHz). Chemical shifts are reported in parts per million (δ-scale), and coupling constants (J) are reported in Hz by using, in the case of ^1H NMR spectroscopy, tetramethylsilane (TMS) or sodium 2,2,3,3-tetradeutero-3-(trimethylsilyl)propionate (TSPNa) as an internal standard and, in the case of ^{13}C NMR spectra, solvent residual peak was taken as reference: $CDCl_3$ at 77.0 ppm, d6-DMSO (dimethyl sulfoxide) at 39.5 ppm, and CD_3OD in D_2O at 49.5 ppm. Standard and peak multiplicities are designated as follows: s (singlet), d (doublet), dd (doublet of doublets), t (triplet), q (quartet), qn (quintet), m (multiplet), br (broad signal). MS data (m/z (%), EI, 70 eV) were obtained by using an Agilent Technologies 5975 spectrometer and a Hewlett-Packard HP5988A quadrupole mass spectrometer operating in electronic ionization (EI) mode at 70 eV and at 4 kV accelerating potential, or a Bruker Biotoff II spectrometer operating in electrospray ionization (ESI) mode with a time of flight (TOF) detector. High-resolution mass spectrometry (HRMS) data were obtained by using a VG AutoSpec (Micromass Instruments) Trisector EBE high-resolution spectrometer (EI mode), a Bruker Biotof II mass spectrometer (ESI-TOF mode), or a Bruker Autoflex spectrometer (MALDI-TOF mode, HCCA matrix). Elemental microanalyses were

dx.doi.org/10.1021/jm300862u | J. Med. Chem. 2012, 55, 7560−7570

obtained on a Carlo−Erba CHNS-O/EA 1108 analyzer. Specific optical rotations ($[\alpha]_D$) were measured with a Perkin-Elmer 241 polarimeter. Sodium D line (589 nm) and a path length of 1 dm were used for measuring at room temperature. The purity of each tested compound (>95%) was determined on an Agilent 1200 LC instrument using a XTerra RP18 column (125 Å, 5 μm, 3 mm × 250 mm, with a flow rate of 0.75 mL/min and detection at 220 nm) using a 95:5 mixture of (NaH_2PO_4, pH = 7 + 0.1% acetonitrile)/(acetonitrile/MeOH 75:25) as eluent.

(*S*)-*N*-(3-(2-Pipecolin-1-yl)propyl)phthalimide (6(*S*)). A solution of 0.41 mL (0.34 g, 3.3 mmol) of (*S*)-(+)-2-methylpiperidine (**4**(*S*)) in 10 mL of acetonitrile was treated with 0.82 g (3.0 mmol) of *N*-(3-bromopropyl)phthalimide (**5**) and 0.70 g (5.0 mmol) anhydrous K_2CO_3 for 8 h at reflux. After concentration, the residue was diluted with 30 mL CH_2Cl_2 and washed with water. The organic layers were combined, dried over anhydrous $MgSO_4$, filtered, and concentrated to give **6**(*S*) as a yellow oil (0.79 g; 92%). IR (film) ν (cm^{-1}): 2931, 2854, 2790, 1772, 1712 (C═O), 1396, 1032 (C−N), 720. ^{1}H NMR (400 MHz, $CDCl_3$) δ (ppm): 7.84 (dd, ^3J = 5.5 Hz, ^4J = 3.0 Hz, 2H, H−C6), 7.71 (dd, ^3J = 5.5 Hz, ^4J = 3.0 Hz, 2H, H−C7), 3.70 (m, 2H, H−C1), 2.78 (m, 2H, H−C3, H−C1a), 2.38 (m, 1H, H−C3), 2.24 (m, 1H, H−C5a), 2.09 (m, 1H, H−C1a), 1.85 (qn, ^3J = 7.5, 2H, H−C2), 1.62−1.42 (m, 4H, H−C2a, H−C3a, H−C4a), 1.24 (m, 2H, H−C3a, H−C4a), 1.03 (d, J = 6.5 Hz, 3H, H−C6a). ^{13}C NMR (100.6 MHz, $CDCl_3$) δ (ppm): 168.3 (C4), 133.8 (C7), 132.2 (C5), 123.1 (C6), 55.8 (C5a), 51.8 (C3), 51.4 (C1a), 36.7 (C1), 34.5 (C4a), 26.1 (C2), 24.6 (C2a), 23.8 (C3a), 18.7 (C6a). MS (ESI-TOF) m/z (%): 287.2 (100) [M^++H], 214.1 (2), 158.0 (5), 141.0 (4), 105.0 (6). HRMS (ESI-TOF) calculated for $C_{17}H_{23}N_2O_2$ [M+1]$^+$: 287.1754; found: 287.1750. Anal. calculated for $C_{17}H_{22}N_2O_2$: C 71.30, H 7.74, N 9.78; found: C 70.95, H 8.03, N 9.78.

(*R*)-*N*-(3-(2-Pipecolin-1-yl)propyl)phthalimide (6(*R*)). A solution of (*R*)-(+)-2-methylpiperidine hydrochloride (**4**(*R*)·HCl) in 10% NaOH was extracted with CH_2Cl_2 to obtain the free amine **4**(*R*). A solution of 0.83 g (8.3 mmol) of (*R*)-(+)-2-methylpiperidine (**4**(*R*)) in 20 mL acetonitrile was treated with 1.65 g (6.0 mmol) *N*-(3-bromopropyl)phthalimide (**5**) and 1.50 g (11 mmol) of anhydrous K_2CO_3 for 8 h at reflux. After concentration, the residue was diluted with 30 mL CH_2Cl_2 and washed with water. The organic layers were combined, dried over anhydrous $MgSO_4$, filtered, and concentrated to give **6**(*R*) as a yellow oil (1.67 g; 97%). IR (film) ν (cm^{-1}): 2930, 2856, 2791, 1772, 1713 (C═O), 1378, 1031 (C−N), 720. ^{1}H NMR (400 MHz, $CDCl_3$) δ (ppm): 7.84 (m, 2H, H−C6), 7.71 (m, 2H, H−C7), 3.70 (m, 2H, H−C1), 2.77 (m, 2H, H−C1a, H−C3), 2.38 (m, 1H, H−C3), 2.26 (m, 1H, H−C5a), 2.10 (dt, ^2J = 10.0 Hz, ^3J = 4.0 Hz, 1H, H−C1a), 1.85 (qn, ^3J = 7.5, 2H, HC2), 1.64−1.43 (m, 4H, H−C2a, H−C3a, HC4a), 1.24 (m, 2H, H−C3a, H−C4a), 1.03 (d, J = 6.5 Hz, 3H, H−C6a). ^{13}C NMR (100.6 MHz, $CDCl_3$) δ (ppm): 168.3 (C4), 133.8 (C7), 132.2 (C5), 123.1 (C6), 55.8 (C5a), 51.8 (C3), 51.4 (C1a), 36.7 (C1), 34.5 (C4a), 26.1 (C2), 24.6 (C2a), 23.8 (C3a), 18.7 (C6a).

(*S*)-*N*-(3-Aminopropyl)-2-pipecoline (3(*S*)). A solution of 0.65 g (2.3 mmol) of (*S*)-*N*-(3-(2-pipecolin-1-yl)propyl)phthalimide (**6**(*S*)) in 10 mL of ethanol was treated with 0.43 mL (8.8 mmol) of hydrazine hydrate under reflux for 1 h. The white precipitate of phthalhydrazide was filtered, and the filtrate was concentrated. After diluting the residue with 5 mL of AcOEt, a new precipitate of phthalhydrazide appeared, which was filtered off. The filtrate was concentrated to dryness to give 0.28 g (1.81 mmol, 79%) of **3**(*S*) as a pale yellow oil. IR (film) ν (cm^{-1}): 3293 (N−H), 2930, 2855, 2788, 1575, 1470, 1374, 1329. ^{1}H NMR (400 MHz, $CDCl_3$) δ (ppm): 2.87 (m, 1H, H−C3), 2.72 (m, 3H, H−C1, H−C1a), 2.35 (m, 1H, H−C3), 2.26 (m, 1H, H−C5a), 2.12 (m, 1H, H−C1a), 1.80−1.50 (m, 8H, H−C2, H−C2a, H−C3a, H−C4a, NH_2), 1.28 (m, 2H, H−C3a, H−C4a), 1.06 (d, ^3J = 6.0 Hz, 3H, H−C6a). ^{13}C NMR (100.6 MHz, $CDCl_3$) δ (ppm): 55.9 (C5a), 52.0 (C3), 51.7 (C1a), 41.0 (C1), 34.6 (C4a), 29.4 (C2), 26.1 (C2a), 23.9 (C3a), 19.0 (C6a). MS (EI) m/z (%): 156.2 (7) [M]$^+$, 112.2 (100), 98.2 (100). HRMS (EI) calculated for $C_9H_{20}N_2$ [M]$^+$: 156.1626; found: 156.1621.

(*R*)-*N*-(3-Aminopropyl)-2-pipecoline (3(*R*)). As described above for **3**(*S*) but using 0.74 g (2.6 mmol) of (*R*)-*N*-(3-(2-pipecolin-1-yl)propyl)phthalimide (**6**(*R*)) in 10 mL of ethanol and 0.50 mL (10 mmol) of hydrazine hydrate to give 0.30 g (1.9 mmol, 73%) of **3**(*R*) as a yellow oil. IR (film) ν (cm^{-1}): 3273 (N−H), 2930, 2855, 2789, 1576, 1472, 1374, 1329. ^{1}H NMR (400 MHz, $CDCl_3$) δ (ppm): 2.86 (dt, ^2J = 11.5 Hz, ^3J = 4.0 Hz, 1H, H−C3), 2.73 (m, 3H, H−C1, H−C1a), 2.35 (m, 1H, H−C3), 2.26 (m, 1H, H−C5a), 2.11 (dt, ^2J = 11.0 Hz, ^3J = 3.0 Hz, 1H, H−C1a), 1.67−1.51 (m, 8H, H−C2, H−C2a, H−C3a, H−C4a, NH_2), 1.27 (m, 2H, H−C3a, H−C4a), 1.06 (d, ^3J = 6.0 Hz, 3H, H−C6a). ^{13}C NMR (100.6 MHz, $CDCl_3$) δ (ppm): 55.9 (C5a), 52.1 (C3), 51.8 (C1a), 41.0 (C1), 34.7 (C4a), 29.5 (C2), 26.2 (C2a), 24.0 (C3a), 19.1 (C6a). MS (EI) m/z (%): 156.1 (2) [M]$^+$, 112.2 (100), 98.1 (68). HRMS (EI) calculated for $C_9H_{20}N_2$ [M]$^+$: 156.1626; found: 156.1624.

(*S*)-*N*,*N*′-(1,4-Phenylenebis(methylene))bis(3-((*S*)-2-methylpiperidin-1-yl)propan-1-amine) Tetrahydrochloride (11(*S*,*S*)). Terephthalaldehyde (**7**) (0.10 g (0.71 mmol)), 0.23 g (1.45 mmol) of (*S*)-*N*-(3-aminopropyl)-2-pipecoline (**3**(*S*)) and Na_2SO_4 were mixed in 6 mL of anhydrous MeOH, and the mixture was heated at reflux under N_2 atmosphere for 24 h. The solid was filtered, and the intermediate imine in MeOH was cooled to 0 °C and treated with 0.06 g (1.45 mmol) of solid $NaBH_4$. The reaction mixture was stirred at room temperature overnight. Then water was added, and the product was extracted with CH_2Cl_2. The organic layers were combined, washed with brine, dried over anhydrous $MgSO_4$, filtered, and concentrated to give 0.29 g (0.67 mmol, 97%) of **1**(*S*,*S*) as a yellow oil. IR (film) ν (cm^{-1}): 3282 (N−H), 2929, 2854, 2793, 1449, 1372. ^{1}H NMR (400 MHz, $CDCl_3$): δ (ppm) 7.30 (m, 4H, H−C2b), 3.79 (d, 4H, H−Cα), 2.92 (m, 2H, H−C1a), 2.79 (m, 2H, H−C3), 2.68 (m, 4H, H−C1), 2.44−2.33 (m, 8H, H−C3, H−C5a, H−C1a), 2.16 (m, 2H, NH), 1.80−1.48 (m, 12H, H−C2, H−C2a, H−C4a, H−C3a), 1.29 (m, 4H, H−C4a, H−C3a), 1.07 (d, 6H, ^3J = 8.0 Hz, H−C6a). ^{13}C NMR (100.6 MHz, $CDCl_3$) δ (ppm): 138.7 (C1b), 127.8 (C2b), 55.8 (C5a), 53.6 (Cα), 52.2 (C3), 52.1 (C1a), 48.2 (C1), 34.7 (C4a), 26.2 (C2a), 25.7 (C2), 23.9 (C3a), 19.1 (C6a). MS (CI) m/z (%): 415.3 (100), 258.2 (42), 112.0 (51). HRMS (CI) calculated for $C_{26}H_{47}N_4$ [M+1]$^+$: 415.3801; found: 415.3811. **1**(*S*,*S*) was converted to the corresponding tetrahydrochloride **11**(*S*,*S*) in almost quantitative yield upon treatment with methanolic HCl in excess followed by concentration of the resulting solution. $[\alpha]_D$ = +15.3 (c = 1.03, MeOH). IR (KBr) ν (cm^{-1}): 3412, 2942, 2745, 1449, 553. ^{1}H NMR (400 MHz, D_2O): δ (ppm) 7.58 (s, 4H, H−C2b), 4.32 (s, 4H, H−Cα), 3.73−3.51 (m, 2H, H−C1a), 3.41−2.98 (m, 12H, H−C1, H−C3, H−C5a, H−C1a), 2.26−1.52 (m, 16H, H−C2, H−C2a, H−C3a, H−C4a), 1.34 (d, 6H, ^3J = 4.0 Hz, H−C6a). ^{13}C NMR (100.6 MHz, D_2O) δ (ppm): 132.6 (C1b), 131.3 (C2b), 60.7 (C5a), 53.0 (Cα), 51.4 (C3), 50.0 (C1a), 44.8 (C1), 32.1 (C4a), 23.6 (C2a), 22.0 (C2), 20.7 (C3a), 17.8 (C6a). Anal. calculated for $C_{26}H_{50}N_4Cl_4$·0.5H_2O: C 54.83, H 9.03, N 9.84; found: C 54.50, H 9.37, N 9.51.

(*R*)-*N*,*N*′-(1,4-Phenylenebis(methylene))bis(3-((*R*)-2-methylpiperidin-1-yl)propan-1-amine) Tetrahydrochloride (11(*R*,*R*)). As above for **1**(*S*,*S*) but using 0.07 g (0.48 mmol) of terephthalaldehyde (**7**), 0.15 g (0.96 mmol) of (*R*)-*N*-(3-aminopropyl)-2-pipecoline (**3**(*R*)), and 0.04 g (0.96 mmol) of solid $NaBH_4$ to give 0.17 g (0.4 mmol, 83%) of **1**(*R*,*R*) as a yellow oil. ^{1}H NMR (400 MHz, $CDCl_3$): δ (ppm) 7.31 (s, 4H, H−C2b), 3.79 (d, 4H, H−Cα), 2.91 (m, 2H, H−C1a), 2.78 (m, 2H, H−C3), 2.68 (m, 4H, H−C1), 2.43−2.32 (m, 8H, H−C3, H−C5a, H−C1a), 2.16 (m, 2H, NH), 1.79−1.49 (m, 12H, H−C2, H−C2a, H−C3a, H−C4a), 1.28 (m, 4H, H−C4a, H−C3a), 1.07 (d, 6H, ^3J = 8.0 Hz, H−C6a). MS (CI) m/z (%): 415.3 (100), 258.1 (31), 112.0 (53). HRMS (CI): calculated for $C_{26}H_{47}N_4$ [M+1]$^+$: 415.3801; found: 415.3800. **1**(*R*,*R*) was converted to the corresponding tetrahydrochloride **11**(*R*,*R*) in almost quantitative yield upon treatment with methanolic HCl in excess followed by concentration of the resulting solution. $[\alpha]_D$ = −16.3 (c = 1.01, MeOH). IR (KBr) ν (cm^{-1}): 3423, 2943, 2743, 1451, 553. ^{1}H NMR (400 MHz, D_2O): δ (ppm) 7.59 (s, 4H, H−C2b), 4.33 (s, 4H, H−Cα), 3.73−3.52 (m, 2H, H−C1a), 3.42−3.00 (m, 12H, H−C1, H−C3, H−C5a, H−C1a), 2.26−1.52 (m, 16H, H−C2, H−C2a, H−C3a, H−C4a), 1.37 (d, 6H, ^3J = 8.0 Hz, H−C6a). ^{13}C NMR (100.6 MHz, D_2O) δ (ppm): 132.6 (C1b), 131.3 (C2b), 60.7 (C5a), 53.0 (Cα), 51.4 (C3), 50.0 (C1a), 44.8 (C1), 32.1 (C4a), 23.6 (C2a), 22.0 (C2), 20.7 (C3a), 17.8 (C6a). Anal. calculated for $C_{26}H_{50}N_4Cl_4$·0.5H_2O: C 54.83, H 9.03, N 9.84; found: C 54.55, H 9.28, N 9.51.

dx.doi.org/10.1021/jm300862u | J. Med. Chem. 2012, 55, 7560−7570

(*S*)-*N*-(4-(Diethoxymethyl)benzyl)-3-(2-methylpiperidin-1-yl)propan-1-amine (9(*S*)). 4-(Diethoxymethyl)benzaldehyde (**8**) (0.35 g (1.6 mmol)), 0.25 g (1.6 mmol) of (*S*)-*N*-(3-aminopropyl)-2-pipecoline (**3**(*S*)), and Na_2SO_4 were mixed in 5 mL of anhydrous MeOH, and the mixture was held at reflux under N_2 atmosphere for 24 h. The solid was filtered and the intermediate imine in MeOH was cooled to 0 °C and treated with 0.056 g (1.45 mmol) of solid $NaBH_4$. The reaction mixture was stirred at room temperature overnight. Then water was added, and the product was extracted with CH_2Cl_2. The organic layers were combined, washed with brine, dried over anhydrous $MgSO_4$, filtered, and concentrated to give 0.47 g (1.3 mmol, 84%) of the **9**(*S*) as a brown oil. IR (film) ν (cm^{-1}): 3283 (N−H), 2973, 2930, 2798, 1663 (C═C), 1444, 1371, 1114, 1055. ^{1}H NMR (400 MHz, $CDCl_3$): δ (ppm) 7.44 (m, 2H, H−C3b), 7.34 (m, 2H, H−C2b), 5.49 (s, 1H, H−C5b), 3.82 (d, ^3J = 9.0 Hz, 2H, H−Cα), 3.72−3.44 (m, 4H, H−C6b), 2.94 (m, 1H, H−C1a), 2.83 (m, 1H, H−C3), 2.71 (m, 2H, H−C1), 2.48−2.36 (m, 3H, H−C3, H−C5a, C1a), 2.21 (m, 1H, NH), 1.84−1.55 (m, 8H, H−C2, H−C2a, H−C3a, H−C4a), 1.24 (m, 6H, H−C7b), 1.09 (d, ^3J = 6.5 Hz, 3H, H−C6a). ^{13}C NMR (100.6 MHz, $CDCl_3$) δ (ppm): 140.1 (C1b), 137.8 (C4b), 127.9 (C2b), 126.7 (C3b), 101.4 (C5b), 64.7 (C5a), 61.0 (C6b), 56.0 (C1a), 53.6 (C3), 52.2 (C1), 48.2 (Cα), 34.4 (C4a), 25.9 (C2), 25.5 (C2a), 23.8 (C3a), 18.9 (C6a), 15.1 (C7b). MS (EI) *m*/*z* (%): 348 (3), 303 (6), 165 (14), 155 (11), 126 (15), 112 (100), 98 (34), 91 (12). HRMS (CI) calculated for $C_{21}H_{36}N_2O_2$ $[M]^+$: 348.2777; found: 348.2778.

(*S*)-4-((3-(2-Methylpiperidin-1-yl)propylamino)methyl)-benzaldehyde (10(*S*)) . The intermediate aminoacetal **9**(*S*) (0.50 g (1.42 mmol)) was treated with 5 mL of 2 M HCl at room temperature for 2 h. The resulting mixture was basified with NaOH and extracted with CH_2Cl_2. The organic layers were combined, washed with brine, dried over anhydrous $MgSO_4$, filtered, and concentrated to give 0.32 g (1.14 mmol, 80%) of the desired product **10**(*S*) as a brown oil. IR (film) ν (cm^{-1}): 3281 (N−H), 2929, 2852, 2797, 2729, 1701 (C═O), 1606 (C═C), 1444, 1371, 1209. ^{1}H NMR (400 MHz, $CDCl_3$): δ (ppm) 10.00 (s, 1H, H−C5b), 7.84 (d, ^3J = 8.0 Hz, 2H, H−C3b), 7.50 (d, ^3J = 8.0 Hz, 2H, H−C2b), 3.87 (s, 2H, H−Cα), 2.90 (m, 1H, H−C1a), 2.79 (m, 1H, H−C3), 2.66 (t, ^3J = 7.0 Hz, 2H, H−C1), 2.42−2.36 (m, 2H, H−C3, H−C5a), 2.20−1.96 (m, 2H, H−C1a, NH), 1.75−1.55 (m, 6H, H−C2, H−C2a, H−C4a, H−C3a), 1.34−1.24 (m, 2H, H−C4a, H−C3a), 1.09 (d, ^3J = 6.5 Hz, 3H, H−C6a). ^{13}C NMR (100.6 MHz, $CDCl_3$) δ (ppm): 192.0 (C5b), 147.8 (C1b), 135.3 (C4b), 129.9 (C3b), 128.5 (C2b), 56.1 (C5a), 53.7 (Cα), 52.3 (C3), 52.0 (C1a), 48.5 (C1), 34.5 (C4a), 26.0 (C2a), 25.8 (C2), 23.8 (C3a), 18.9 (C6a). MS (EI) *m*/*z* (%): 274 (6), 183 (3), 155 (7), 126 (9), 119 (10), 112 (100), 98 (39), 91 (14). HRMS (EI) calculated for $C_{17}H_{26}N_2O$ $[M]^+$: 274.2045; found: 274.2037.

3-((*R*)-2-Methylpiperidin-1-yl)-*N*-(4-((3-((*S*)-2-methylpiperidin-1-yl)propylamino)methyl)benzyl)propan-1-amine Tetrahydrochloride (11(*S*,*R*)). (*S*)-4-((3-(2-Methylpiperidin-1-yl)-propylamino)methyl)benzaldehyde (**10**(*S*)) (0.32 g (1.14 mmol)), 0.18 g (1.44 mmol) of (*R*)-*N*-(3-aminopropyl)-2-pipecoline (**3**(*R*)), and Na_2SO_4 were mixed in 8 mL of anhydrous MeOH, and the mixture was heated at reflux under N_2 atmosphere for 24 h. The solid was filtered, and the intermediate imine in MeOH was cooled to 0 °C and treated with 0.05 g (1.14 mmol) of solid $NaBH_4$. The reaction mixture was stirred at room temperature overnight. Then water was added, and the product was extracted with CH_2Cl_2. The organic layers were combined, washed with brine, dried over anhydrous $MgSO_4$, filtered, and concentrated to give 0.40 g (0.95 mmol, 83%) of **1**(*S*,*R*) as a yellow oil. ^{1}H NMR (400 MHz, $CDCl_3$): δ (ppm) 7.30 (s, 4H, H−C2b), 3.79 (d, 4H, H−Cα), 2.89 (m, 2H, H−C1a), 2.77 (m, 2H, H−C3), 2.67 (m, 4H, H−C1), 2.41−2.27 (m, 8H, H−C3, H−C5a, H−C1a), 2.16 (m, 2H, NH), 1.75−1.48 (m, 12H, H−C2, H−C2a, H−C4a, H−C3a), 1.29 (m, 4H, H−C4a, H−C3a), 1.06 (d, 6H, ^3J = 8.0 Hz, H−C6a). HRMS (CI) calculated for $C_{26}H_{47}N_4$ $[M+1]^+$: 415.3801; found: 415.3803. **1**(*S*,*R*) was converted to the corresponding tetrahydrochloride **11**(*S*,*R*) in almost quantitative yield upon treatment with methanolic HCl in excess followed by concentration of the resulting solution. $[\alpha]_D$ = 0.00 (*c* = 1.03, MeOH). IR (KBr) ν (cm^{-1}): 3446, 2944, 2681, 1456, 526. ^{1}H NMR (400 MHz, D_2O): δ (ppm) 7.59 (s, 4H, H−C2b), 4.33 (s, 4H, H−Cα), 3.74−3.52 (m, 2H, H−C1a), 3.42−2.98 (m, 12H, H−C1, H−C3, H−C5a, H−C1a), 2.27−1.51 (m, 16H, H−C2, H−C2a, H−C3a, H−C4a), 1.37 (d, 6H, ^3J = 8.0 Hz, H−C6a). ^{13}C NMR (100.6 MHz, D_2O) δ (ppm): 132.6 (C1b), 131.3 (C2b), 60.7 (C5a), 53.0 (Cα), 51.4 (C3), 50.0 (C1a), 44.8 (C1), 32.1 (C4a), 23.6 (C2a), 22.0 (C2), 20.7 (C3a), 17.8 (C6a). Anal. calculated for $C_{26}H_{50}N_4Cl_4 \cdot 0.5H_2O$: C 54.83, H 9.03, N 9.84; found: C 55.06, H 9.35, N 9.52.

Biology. *(A). Antiviral Activity.* HIV-1 strains were titered in MT-4 cells after acute infection, and infectivity was measured by evaluating the cytopathic effect that was induced after 5-day cultures as described.[22] Anti-HIV activity (EC_{50}) and cytotoxicity (CC_{50}) measurements in MT-4 cells were based on the viability of cells that had been infected or not infected with HIV-1; all were exposed to various concentrations of the test compound. After the MT-4 cells were allowed to proliferate for 5 days, the number of viable cells was quantified by a tetrazolium-based colorimetric method (MTT method) as described.

(B). ADME-TOX Studies. The multigram quantities of **11**, **11**(*R*,*R*), **11**(*S*,*S*), and **11**(*S*,*R*) necessary for the ADME-Tox studies were prepared by ENANTIA S.L. (http://www.enantia.com).

In Vitro Human CXCR4 Receptor Functional Assay. This functional assay was determined at CEREP (http://www.cerep.fr). The CXCR4 (antagonist effect), test (ref. 2466), was determined using human recombinant (CHO) cells following the protocol described by Zhou et al.[18] Stimulant, SDF-1a; stimulant concentration, 1 nM; measured component, impedance; incubation, 28 °C; detection method, cellular dielectric spectroscopy; reference compound, MIP-II (IC_{50} = 55 nM).

Cardiac Toxicity Assays (hERG). Determined at CEREP (http://www.cerep.fr), hERG (automated patch-clamp) test (ref. 2245), using hERG CHO-K1 cell line by following the automated patch-clamp methodology proposed by Mathes.[19] Test concentration, 0.1, 1, 10 μM; incubation, 5 min/room temperature, cumulatively; detection method, automated whole-cell patch-clamp; reference, E-4031 (IC_{50} = 25.6 nM).

Acute Intravenous Toxicity Study in Mice: Determination of Maximum Nonlethal Dose and Minimum Lethal Dose. Determined at Harlan Laboratories S.A. (http://www.harlan.com/). The acute toxicity of the test items AMD3100, **11**(*R*,*R*), **11**(*S*,*S*), and **11**(*S*,*R*) was evaluated after their intravenous administration to Hsd:ICR (CD-1) mice (vehicle: physiological saline solution, sodium chloride 0.9%, B. Braun Medical, S.A.) followed by an observation period of 14 days. The animals received a single dose of the test item by intravenous injection in the lateral vein of the tail using a graduated syringe and a 25G (0.5 × 16 mm) needle. The test item was administered to groups consisting of two males and two females each. In the study, 4 groups consisting of 4 animals (2 males and 2 females) each were administered in physiological saline solution at doses of 1, 2, 3, 3.5, and 4 mg/kg. Viability/mortality: daily during the acclimatization period, during the first 30 min and at approximately 1, 2, 3, and 5 h after administration on test day 1 (in common with the clinical signs) and twice daily during days 2−15. Clinical signs: daily during the acclimatization period, during the first 30 min and at approximately 1, 2, 3, and 5 h after administration on test day 1, and once daily during days 2−15. All abnormalities were recorded. On the basis of the results obtained, the maximum nonlethal dose and the minimum lethal dose of the test items when administered intravenously to Hsd:ICR (CD-1) mice for both sexes as well as for males and females separately were determined.

(C). Effect of CXCR4 Inhibitors on GICs and Glioma Initiation. **Reagents.** CXCL12 was purchased from R&D Systems. Specific antibodies against p-MAPK, MAPK, p-AKT, AKT (all from Cell Signaling), and α-Tubulin (Sigma) were used for immunoblotting.

GBM Neurospheres. GBM neurospheres were generated as described previously.[14] Human GBM specimens were obtained from the Vall d'Hebron Hospital. The clinical protocol was approved by the Vall d'Hebron Institutional Review Board (CEIC), with informed consent obtained from all subjects.

Proliferation Assay. Neurosphere cultures were dissociated with acutase during 3 min, and then cells were counted. An equal number of cells was seeded in triplicate for each condition and treated or left untreated with CXCR4 inhibitors (1 μM) and/or CXCL12 (10 ng/

mL). Media and treatments were refreshed every 2−3 days. After 7 days cells were collected, dissociated with acutase, stained with tripan blue, and counted with a Countess Automated Cell Counter (Invitrogen).

Analysis of the CD44+ Population by Flow Cytometry. GBM neurospheres were dissociated and individual cells were incubated for 15 min in blocking solution containing 10 μg/mL human IgG, followed by anti-CD44 antibody or the control IgG2b isotype, both FITC-conjugated (BD Pharmingen). Cells were incubated for 20 min on ice protected from light, washed in phosphate-buffered saline (PBS), and stained with propidium iodide (Sigma) to discriminate dying cells. Cells were then analyzed by flow cytometry (FACSCalibur; Beckton Dickinson) or sorted (MoFlo; DAKO) after staining with CD44-FITC.

Intracranial Tumor Assay. All mouse experiments were approved by and performed according to the guidelines of the Institutional Animal Care Committee of the Vall d'Hebron Research Institute in agreement with the European Union and national directives. Cells were collected, dissociated with acutase, stained with trypan blue to assess viability, and counted with a Countess Automated Cell Counter (Invitrogen). Live cells (100.000) were stereotactically inoculated into the corpus striatum of the right-brain hemisphere (1 mm anterior and 1.8 mm lateral to the bregma; 2.5 mm intraparenchymal) of 9-week-old NOD-SCID mice (Charles River Laboratories). Mice were euthanized when they presented neurological symptoms or a significant loss of weight. Magnetic resonance imaging (MRI) analysis was performed in mice injected intraperitoneally with gadolinium diethylenetriamine pentaacetic acid at a dose of 0.25 mmol of gadolinium/kg of body weight. T1W magnetic resonance images were acquired in a 9.4 T vertical bore magnet interfaced to an AVANCE 400 system (Bruker) using a spin−echo sequence as described previously.[14]

■ ASSOCIATED CONTENT

Ⓢ Supporting Information

Spectral data for compounds **6**(*S*), **6**(*R*), **3**(*S*), **3**(*R*), **1**(*S,S*), **11**(*S,S*), **1**(*R,R*), **11**(*R,R*), **9**(*S*), **10**(*S*), and **11**(*S,R*). High-performance liquid chromatography (HPLC) analytical profile for **11**(*S,S*), **11**(*R,R*), and **11**(*S,R*). CD44 low/CD44 null analysis. This material is available free of charge via the Internet at http://pubs.acs.org.

■ AUTHOR INFORMATION

Corresponding Author

*Dr. José I. Borrell: phone, +34 932 672 059; fax, +34 932 056 266; e-mail, j.i.borrell@iqs.url.edu. Dr. Joan Seoane: phone, +34 934 894 167; fax, +34 934 893 884; e-mail jseoane@vhio.net.

Notes

The authors declare the following competing financial interest(s): L. Ros-Blanco, J. Esté, J. Teixidó, and J. I. Borrell are co-inventors of patents WO 2008/049950 A1 and PCT/ES2011/070407 covering the compounds and their use, licensed to Janus Development SL.

■ ACKNOWLEDGMENTS

The authors appreciate the financial support from Janus Development SL, which also contributed to the ADME-TOX and GICs/glioma initiation studies design. We also appreciate the financial support from the Spanish Ministerio de Economía y Competitividad project SAF2010-C21617-C02 (J.I.B. and B.C.) and BFU2009-06958 (J.A.E.). L.R.-B. thanks IQS and Generalitat de Catalunya for a scholarship and a FI−B 2008−2010 scholarship, respectively.

■ ABBREVIATIONS USED

Akt, protein kinase B; CC_{50}, half cytotoxic concentration; CXCL12, chemokine (C−X−C motif) ligand 12; CXCR4, CXC chemokine receptor type 4; EC_{50}, 50% effective concentration; GBM, grade IV gliomas or glioblastoma; GICs, glioma initiating cells; hERG, human Ether-à-go-go-Related Gene; HIV-1, human immunodeficiency virus type 1; MAPK, mitogen-activated protein kinase; MLD, minimum lethal dose; MND, maximum nonlethal dose; MRI, magnetic resonance imaging; p-Akt, phospho-Akt; p-MAPK, phospho-MAPK; PI3K, phosphatidylinositol 3-kinase

■ REFERENCES

(1) Brat, D. J.; Castellano-Sanchez, A. A.; Hunter, S. B.; Pecot, M.; Cohen, C.; Hammond, E. H.; Devi, S. N.; Kaur, B.; Van Meir, E. G. Pseudopalisades in Glioblastoma Are Hypoxic, Express Extracellular Matrix Proteases, and Are Formed by an Actively Migrating Cell Population. *Cancer Res.* **2004**, *64*, 920−927.

(2) Furnari, F. B.; Fenton, T.; Bachoo, R. M.; Mukasa, A.; Stommel, J. M.; Stegh, A.; Hahn, W. C.; Ligon, K. L.; Louis, D. N.; Brennan, C.; Chin, L.; DePinho, R. A.; Cavenee, W. K. Malignant astrocytic glioma: Genetics, biology, and paths to treatment. *Genes Dev.* **2007**, *21*, 2683−2710.

(3) Zhu, Y.; Parada, L. F. The molecular and genetic basis of neurological tumours. *Nat. Rev. Cancer* **2002**, *2*, 616−626.

(4) Anido, J.; Sáez-Borderías, A.; Gonzàlez-Juncà, A.; Rodón, L.; Folch, G.; Carmona, M. A.; Prieto-Sánchez, R. M.; Barba, I.; Martínez-Sáez, E.; Prudkin, L.; Cuartas, I.; Raventós, C.; Martínez-Ricarte, F.; Poca, M. A.; García-Dorado, D.; Lahn, M. M.; Yingling, J. M.; Rodón, J.; Sahuquillo, J.; Baselga, J.; Seoane, J. TGF-beta Receptor Inhibitors Target the CD44(high)/Id1(high) Glioma-Initiating Cell Population in Human Glioblastoma. *Cancer Cell* **2010**, *18*, 655−668.

(5) Visvader, J. E.; Lindeman, G. J. Cancer stem cells in solid tumours: Accumulating evidence and unresolved questions. *Nat. Rev. Cancer* **2008**, *8*, 755−768.

(6) Este, J. A.; Telenti, A. HIV entry inhibitors. *Lancet* **2007**, *370*, 81−88.

(7) Tilton, J. C.; Doms, R. W. Entry inhibitors in the treatment of HIV-1 infection. *Antiviral Res.* **2010**, *85*, 91−100.

(8) Pettersson, S.; Pérez-Nueno, V. I.; Ros-Blanco, L.; Puig de La Bellacasa, R.; Rabal, M. O.; Batllori, X.; Clotet, B.; Clotet-Codina, I.; Armand-Ugón, M.; Esté, J. A.; Borrell, J. I.; Teixidó, J. Discovery of novel non-cyclam polynitrogenated CXCR4 coreceptor inhibitors. *ChemMedChem* **2008**, *3*, 1549−1557.

(9) Bian, X. W.; Yang, S. X.; Chen, J. H.; Ping, Y. F.; Zhou, X. D.; Wang, Q. L.; Jiang, X. F.; Gong, W.; Xiao, H. L.; Du, L. L.; Chen, Z. Q.; Zhao, W.; Shi, J. Q.; Wang, J. M. Preferential expression of chemokine receptor CXCR4 by highly malignant human gliomas and its association with poor patient survival. *Neurosurgery* **2007**, *61*, 570−578.

(10) Tseng, D.; Vasquez-Medrano, D. A.; Brown, J. M. Targeting SDF-1/CXCR4 to inhibit tumour vasculature for treatment of glioblastomas. *Br. J. Cancer* **2011**, *104*, 1805−1809.

(11) Teicher, B. A.; Fricker, S. P. CXCL12 (SDF-1)/CXCR4 pathway in cancer. *Clin. Cancer Res.* **2010**, *16*, 2927−2931.

(12) Terasaki, M.; Sugita, Y.; Arakawa, F.; Okada, Y.; Ohshima, K.; Shigemori, M. CXCL12/CXCR4 signaling in malignant brain tumors: A potential pharmacological therapeutic target. *Brain Tumor Pathol.* **2011**, *28*, 89−97.

(13) do Carmo, A.; Patricio, I.; Cruz, M. T.; Carvalheiro, H.; Oliveira, C. R.; Lopes, M. C. CXCL12/CXCR4 promotes motility and proliferation of glioma cells. *Cancer Biol. Ther.* **2010**, *9*, 56−65.

(14) Peñuelas, S.; Anido, J.; Prieto-Sánchez, R. M.; Folch, G.; Barba, I.; Cuartas, I.; García-Dorado, D.; Poca, M. A.; Sahuquillo, J.; Baselga, J.; Seoane, J. TGF-beta increases glioma-initiating cell self-renewal through the induction of LIF in human glioblastoma. *Cancer Cell.* **2009**, *15* (4), 315−327.

(15) Doller, D.; Davies, R.; Chackalamannil, S. A practical preparation of (*R*)- and (*S*)-*N*-Boc-2-methylpiperidines. *Tetrahedron: Asymmetry* **1997**, *8*, 1275−1278.

(16) Apelt, J.; Ligneau, X.; Pertz, H. H.; Arrang, J.; Ganellin, C. R.; Schwartz, J.; Schunack, W.; Stark, H. Development of a new class of nonimidazole histamine H_3 receptor ligands with combined inhibitory

histamine *N*-methyltransferase activity. *J. Med. Chem.* **2002**, *45*, 1128−1141.
(17) Jo, M. N.; Seo, H. J.; Kim, Y.; Seo, S. H.; Rhim, H.; Cho, Y. S.; Cha, J. H.; Koh, H. Y.; Choo, H.; Pae, A. N. Novel T-type calcium channel blockers: Dioxoquinazoline carboxamide derivatives. *Bioorg. Med. Chem.* **2007**, *15*, 365−373.
(18) Zhou, Y.; Larsen, P. H.; Hao, Ch.; Yong, V. W. CXCR4 is a major chemokine receptor on glioma cells and mediates their survival. *J. Biol. Chem.* **2002**, *277*, 49481−49487.
(19) Mathes, C. QPatch: The past, present and future of automated patch clamp. *Expert Opin. Ther. Targets* **2006**, *10*, 319−327.
(20) Sturgill, T. W. MAP kinase: It's been longer than fifteen minutes. *Biochem. Biophys. Res. Commun.* **2008**, *371*, 1−4.
(21) Rubin, J. B.; Kung, A. L.; Klein, R. S.; Chan, J. A.; Sun, Y.; Schmidt, K.; Kieran, M. W.; Luster, A. D.; Segal, R. A. A small-molecule antagonist of CXCR4 inhibits intracranial growth of primary brain tumors. *Proc. Natl. Acad. Sci. U.S.A.* **2003**, *100* (23), 13513−13518.
(22) Gonzalez-Ortega, E.; Ballana, E.; Badia, R.; Clotet, B.; Este, J. A. Compensatory mutations rescue the virus replicative capacity of VIRIP-resistant HIV-1. *Antiviral Res.* **2011**, *92*, 479−483.